OPEN

PRS GLOBAL OPEN

ORIGINAL ARTICLE
Research

TSG-6 Is Involved in Fibrous Structural Remodeling after the Injection of Adipose-derived Stem Cells

Satomi Kiuchi, MS*
Tiago J.S. Lopes, PhD†‡
Takaya Oishi, MS*
Yuki Cho, MS*
Hiroko Ochiai, MD§
Takamasa Gomi, PhD*

Background: Although aesthetic treatments can rejuvenate the skin, they often cause specific forms of tissue damage. Unlike wounding, which typically results in fibrotic scar tissue, damage from aesthetic treatments induces a distinct histological rejuvenation. The mechanisms that drive this rejuvenation are not yet fully understood. Here, we were interested in cellular responses following aesthetic treatments injecting adipose-derived stem cells (ASCs) subcutaneously. Through investigation with an ex vivo experimental model, a key gene was identified that orchestrates fibrous structural changes and tissue remodeling.

Methods: Using fresh human subcutaneous adipose tissue co-cultured with ASCs, the changes in the fibrous architecture of the tissue were sequentially mapped. The key regulatory genes involved in remodeling were identified using gene expression and computational analyses.

Results: We identified the regulatory elements that are crucial for tissue remodeling. Among those, we found that tumor necrosis factor-stimulated gene-6 (TSG-6) is a paracrine mediator essential for the collagen activity. It not only alleviates tissue inflammation but also promotes collagen replacement ex vivo. This is primarily achieved by inhibiting the formation of neutrophil extracellular traps, which are known to promote fibrosis.

Conclusions: TSG-6 is a key factor modulating tissue inflammation. As our results demonstrate, after ASCs treatment, this factor directs skin healing away from fibrosis by reducing neutrophil extracellular trap formation in subcutaneous adipose tissue and promotes fibrous rejuvenation. *(Plast Reconstr Surg Glob Open 2024; 12:e5990; doi: 10.1097/GOX.0000000000005990; Published online 19 July 2024.)*

INTRODUCTION

The human skin is our largest organ and serves multiple roles for human survival. To truly understand the significance of skin and its relation to aging, it is necessary to investigate its intricate structure, especially the fibrous components of the extracellular matrix (ECM). The main components of ECM are collagen, elastin, and proteoglycans, which provide mechanical strength, elasticity, and moisture to the skin.[1] However, chronological aging, coupled with external factors like photodamage, leads to a decline in these essential ECM components or an accumulation of degraded ECM.[2,3] On a macroscopic level, this manifests as the skin wrinkles, sags, and undergoes atrophy, which we often associate with aging.

Although temporary compensation approaches exert some effect for decreased ECM, an accumulation of degraded ECM had been considered difficult to remove except for certain aesthetic treatments by physicians, such as the injection of adipose-derived stem cells (ASCs) subcutaneously. The mechanism is considered not only physical replenishment but also a biological response that removes degraded ECM and replaces them with new ones. This is based on the finding that in treated skin, dermal elastosis is reduced and elastic fibers are regenerated, resulting in a histologically rejuvenated phenotype.[4] Moreover, the ASCs injection treatment also improves skin fibrosis caused by X-irradiation.[5]

Yet, despite the wealth of research showcasing its benefits,[6] studies explaining the underlying mechanisms of the biological responses in the ASCs-injected skin are

*From *POLA Chemical Industries, Inc., Yokohama, Japan; †Center of Regenerative Medicine, National Center for Child Health and Development Research Institute, Tokyo, Japan; ‡Nezu Life Sciences, Karlsruhe, Germany; and §NHO Tokyo Medical Center, Tokyo, Japan*
Received for publication January 10, 2024; accepted May 29, 2024.

DOI: 10.1097/GOX.0000000000005990

Disclosure statements are at the end of this article, following the correspondence information.

Related Digital Media are available in the full-text version of the article on www.PRSGlobalOpen.com.

lacking. Damage to the skin often leads to fibrosis, a far cry from rejuvenation. Therefore, a major question in skin biology is how ASC injection treatment, which intrinsically involves some degree of tissue disruption, avoids the fibrotic response and leads to histological rejuvenation.

In this study, we analyzed the mechanisms driving the observed fibrous structural changes after ASC injection treatment. We identified TSG-6 as a key factor in tissue remodeling, exerting its role by modulating inflammatory states involving neutrophils.

Elucidating the biological mechanisms and a key factor underlying aesthetic treatments may contribute to shortening the recovery time or establishing safer and more effective alternative methods.

Takeaways

Question: Subcutaneous injections of adipose-derived stem cells involve some degree of tissue disruption, but avoid fibrotic response and lead to histological rejuvenation. What is the molecular mechanism underlying this phenomenon?

Findings: TSG-6 is a key factor that modulates the inflammatory state of tissues by inhibiting the formation of the neutrophil extracellular traps in subcutaneous adipose tissue. It drives tissue state from the direction of fibrosis towards fibrous structural remodeling.

Meaning: The modulation of TSG-6 may contribute to shortening the recovery time after aesthetic treatments and allow patients to maximize the rejuvenation effect. It can also contribute to establishing safer and more effective alternative methods.

MATERIALS AND METHODS

Tissue Samples

Abdominal subcutaneous adipose tissues were obtained from Japanese male and female volunteers (age 38–84) at NHO Tokyo Medical Center who had provided consent. Only surplus tissue from abdominal skin excision for grafting purposes was used. The study was approved by the ethical committees of NHOTMC (R17-209, approved March 23, 2018) and POLA Chemical Industries, Inc. (2018-G-032, approved March 8, 2018). The samples were cut into 3- to 6-mm pieces and culture began within a few hours of harvest.

Cheek subcutaneous adipose tissues from White women (age 25–90) were purchased from Obio, LLC. (El Segundo, Calif.).

Cell Culture

In this study, purchased primary cultured normal human ASCs were used to allow for the preparation of ASC cultures before surgical excision of tissue samples. ASCs (PT-5006, Lonza, Basel, Switzerland) were cultured in ADSC Growth Medium BulletKit (PT-4505, Lonza) at 37°C with 5% CO_2. Human neutrophils (PB011C-1, HemaCare, Northridge, Calif.) were cultured in RPMI 1640 Medium (Thermo Fisher Scientific, Waltham, MA) containing 10% FBS (Moregate Biotech, Bulimba, Australia) and 2 mM L-Glutamine (Thermo Fisher Scientific) at 37°C with 5% CO_2.

Ex Vivo Experimental Model

ASCs were preseeded in six-well plates, where fresh tissue samples were cultured in cell inserts at 37°C with 5% CO_2. Initiation of co-cultures was coincided with the carry-in of each tissue sample so that experiments could be performed before biological responses ceased due to tissue deterioration. The media was changed to Dulbecco's Modified Eagle Medium/Ham Nutrient Mixture F-12 (DMEM/F-12) (Merck, Darmstadt, Germany) containing 10% FBS and 2.5× Antibiotic-Antimycotic Mixed Solution (Nacalai tesque, Kyoto, Japan). To inhibit TSG-6 function, 2.5 ng/mL goat anti-TSG-6 antibody (R&D systems, Minneapolis, Minn.) was added to the medium.

Gene Expression Analysis

Total RNA was extracted from tissues with the RNeasy Lipid Tissue Mini Kit (Qiagen, Hilden, Germany). RNA sequencing libraries were generated and sequenced by Azenta Life Sciences (Chelmsford, Mass.) using NovaSeq 6000 (Illumina, San Diego, Calif.). Quality control was performed using FastQC (version 0.10.1).[7] Mapping the reads to the reference genome was performed using HISAT2 (version 2.0.1).[8] Expression levels of mRNAs (fragments per kilobase of exon per million mapped reads) were determined using HT-seq (version 0.6.1).[9] Differential expression analysis was performed using the Bioconductor package DESeq2 (version 1.26.0)[10] (fold change > 1.5 and FDR < 0.05).

Gene ontology (GO) enrichment analysis of differentially expressed genes (DEGs) was performed using Enrichr (version 3.0)[11,12]. The protein–protein interaction (PPI) network of DEGs was constructed using HIPPIE 2.2.[13] Cytoscape (version 3.8.2)[14] was used to visualize the network and calculate the degree centrality.

For qPCR, total RNA was reverse-transcribed into cDNA with Superscript VILO cDNA Synthesis kit (Thermo Fisher Scientific), and cDNA was amplified by QuantiTect SYBR Green PCR Kits (Qiagen). Pre-designed primers were purchased from Qiagen.

Confocal Fluorescence Assay

Each tissue sample was embedded in 2.5% agarose XP (Nippon Gene, Tokyo, Japan) dissolved in sterile PBS. The embedded tissue was flattened by cutting it in half using a razor and placed flattened side down in a culture insert (Merck). A hole was punched at the center of the culture insert with a biopsy (diameter: 3.0 mm; KAI, Tokyo, Japan) so a portion of the flattened tissue was exposed.

To detect collagen degradation, the embedded tissues were stained with 5-μM Cy3-conjugated collagen hybridizing peptide (3Helix, Salt Lake City, Utah) and 1 μg/mL Hoechst 33342 (DOJINDO, Kumamoto, Japan), and incubated for 1 hour. To detect collagen synthesis, the embedded tissues were immunolabeled with rat anti-procollagen type I antibody (1:500, Merck) overnight followed by secondary antibody (Alexa Fluor Plus donkey antirat 488,

1:500, Thermo Fisher Scientific) and 1 μg/mL Hoechst 33342 for 2 hours.

After each staining, the multi-stack images of the embedded tissues were obtained with the laser confocal microscope (A1R+, Nikon, Tokyo, Japan). After observation, tissues were cultured for 7 days, fluorescently stained, and set under observation again. In the second observation, an image of the same area was obtained with the same imaging conditions. The obtained three-dimensional images were projected in two dimensions to create a maximum intensity projection. Using Image J, the RGB images were converted to grayscale and binarized, and the stained area value was calculated. Three-dimensional images were created using Imaris (version 9.2.1, Carl Zeiss, Germany).

Neutrophil Extracellular Traps Induction, Quantification, and Detection

Neutrophils were seeded in poly-D-lysine charged glass coverslips within 24-well plate by centrifugation for 3 minutes at 300× g. The cells were precultured with or without recombinant human TSG-6 protein (31.25-250 pg/mL, R&D systems) for 15 minutes as necessary. Subsequently, the cells were incubated with phorbol-12-myristate-13-acetate (50 nM, FUJIFILM Wako Pure Chemical, Tokyo, Japan) for 1 hour to induce the formation of neutrophil extracellular traps (NETs). The supernatant was collected by centrifugation for 3 minutes at 300× g. When the collected supernatant was used for co-culture with tissue, before centrifugation, cells were washed and replaced with medium to prevent phorbol-12-myristate-13-acetate carryover. Quant-iT PicoGreen dsDNA Assay Kit (Thermo Fisher Scientific) was used to measure the DNA concentration in the NETs. The supernatant prepared at 200 ng/mL of dsDNA was used as a NET-containing medium.

To detect NETs in tissue, the tissues embedded in OCT compound (Sakura Finetek Japan, Tokyo, Japan) were frozen and sliced into sections with a cryostat (POLAR-DM, Sakura Finetek Japan). The sections were fixed with 10% Formalin Neutral Buffer Solution (FUJIFILM Wako Pure Chemical) for 10 minutes, blocked with 1% donkey serum (FUJIFILM Wako Pure Chemical) for 30 minutes, and immunolabeled with primary antibodies overnight followed by secondary antibodies for 1 hour. The primary antibodies used were goat anti-myeloperoxidase (5 μg/mL, R&D systems) as a neutrophil marker, and rabbit anti-histone H3 (citrulline R2 + R8 + R17; 1 μg/mL, Abcam, Cambridge, United Kingdom) as an extracellular trap marker. The secondary antibodies used were Alexa Fluor Plus donkey antigoat 488, and Alexa Fluor Plus donkey antirabbit 555 (Thermo Fisher Scientific). After the immunolabeling, the sections were mounted with ProLong gold antifade mountant with DAPI (Thermo Fisher Scientific). The images of the sections were obtained with a fluorescence microscope (BZ-X800; KEYENCE, Osaka, Japan).

Statistical Analysis

All data are presented as the mean values with the standard error of the mean. Comparisons between two groups were performed with Student *t* test. Comparisons of multiple groups were performed using analysis of variance followed by Tukey honest significant difference (HSD) or Dunnett test. In all cases, *P* values of less than 0.05 were considered statistically significant.

RESULTS

Establishing an Ex Vivo Assay to Obtain Biological Responses

To study the biological responses triggered by ASCs, we developed an ex vivo co-culture model of freshly excised human subcutaneous adipose tissue in conjunction with ASCs. This system ensures cell viability for 7 days,[15] and tissues cultured in the absence of ASCs were used as controls.

To validate our model as a surrogate for post-ASC injection, we examined fibrous structural shifts, focusing on both collagen degradation and synthesis. Utilizing a fluorescent collagen hybridizing peptides probe, which exhibits an affinity for loosened collagen triple strands, we observed a transient augmentation in collagen degradation signals, peaking at day 3 post-ASC co-culture (Fig. 1A). Concurrently, immunofluorescence imaging elucidated a consistent surge in collagen synthesis signals, prominent at day 7 (Fig. 1B).

This episodic pattern (transient collagen degradation superseded by synthesis) leads to a substantive remodeling of the fibrous elements within the subcutaneous adipose tissue. Thus, this model reproduces the different stages of fibrous remodeling orchestrated by ASCs.

Wound Healing Dynamics Can Be Observed in the Experimental Model

To clarify gene expression shifts during wound healing, we collected sample aliquots over time and sequenced their RNA contents. DEGs on days 2, 3, and 7 were isolated in both ASC-present and ASC-absent cultures, and we compared their expression profiles to the genes expressed on day 1 (Fig. 2A). [**See figure, Supplemental Digital Content 1,** which shows a number of DEGs on each culture day against 1 d of culture (DEGs, >1.5-fold changes and <0.05 false discovery rate), shown in Fig. 2. **http://links.lww.com/PRSGO/D354**.] GO annotations showed an increase in the presence of factors associated with cellular proliferation (days 2 and 3) and ECM assembly (day 7) in both assays (Fig. 2B–F).

Interestingly, after day 7, the inflammation dynamics diverged; while the ASC-absent culture showed a continuous increase in the expression of certain inflammation-linked genes (Fig. 2C), the ASC-present culture exhibited a decreased expression of other inflammation-linked genes (Fig. 2E).

In all cultures, these results demonstrate that gene expression analysis reveals a trajectory that resembles the known wound healing phases, namely inflammation, proliferation, and reconstruction[16]; hence, it is appropriate to study the mechanism of this biological phenomenon.

ASCs Expedite the Termination of the Inflammatory Response

To elucidate the impact of ASCs on gene expression within subcutaneous adipose tissue, we compared the

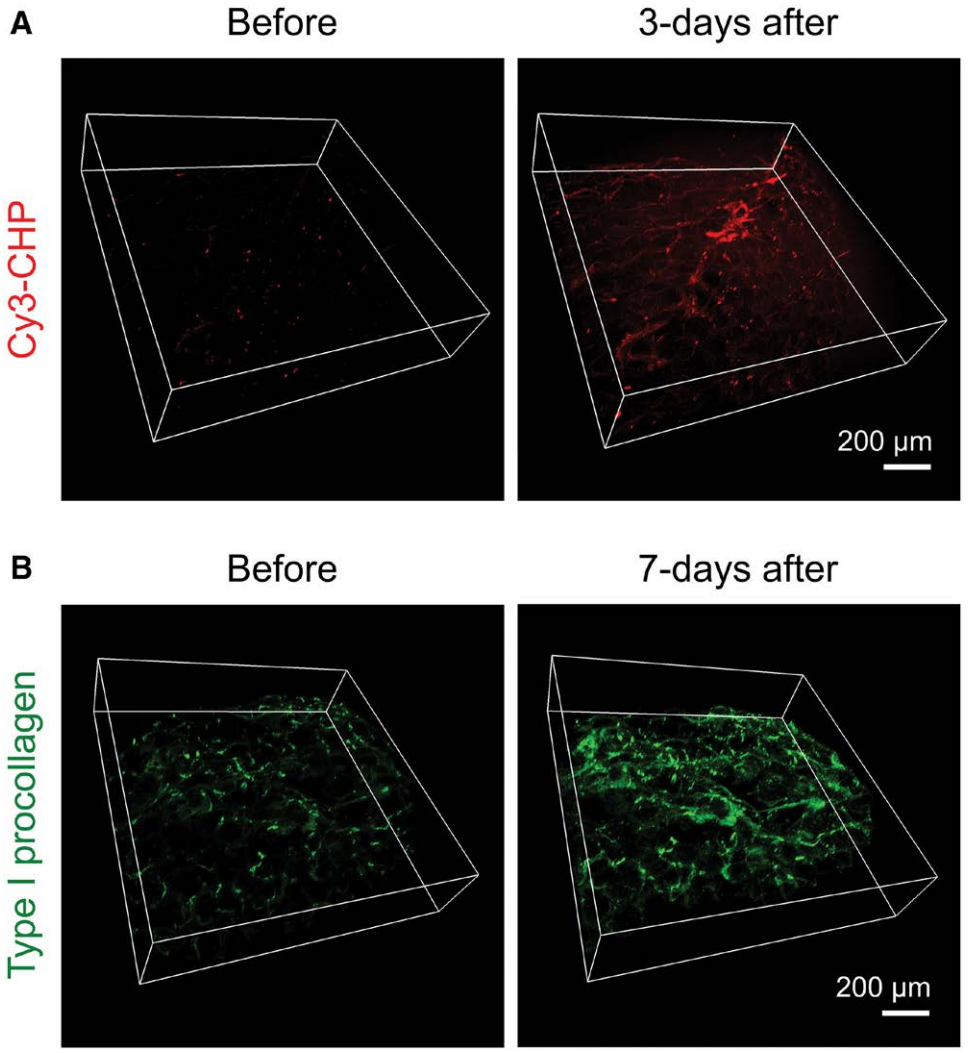

Fig. 1. Establishment of an ex vivo experimental model. A–B, Observation of fibrous structural changes in ex vivo experimental model. Fresh subcutaneous adipose tissue was co-cultured with ASCs, and fluorescent signals of collagen degradation (A) and synthesis (B) of type I collagen were detected in the same areas before and after culture. Each observation was performed for 13 donors, and representative images are shown here. Scale bars = 200 μm.

expression profile of ASC co-cultures with non-ASC control cultures (Fig. 3A). [**See figure, Supplemental Digital Content 2,** which shows a number of DEGs with ASCs compared with without ASCs on each culture day (DEGs, >1.5-fold changes and <0.05 false discovery rate), shown in Fig. 3. **http://links.lww.com/PRSGO/D355**.] Following a day of culture, we observed inhibition of the Notch signaling cascade (a known pro-fibrotic mechanism[17]) and the suppression of muscle and cytoskeletal functional entities, notably α-SMA, a hallmark myofibroblast constituent pivotal to fibrosis.[18] This implicates an early initiation of antifibrotic signaling under ASC influence. By day 3 of co-culture, the expression of genes associated with ECM disassembly, typified by matrix metalloproteinases (MMPs) and analogous catabolic enzymes, increased, whereas those linked to elastic fiber assembly decreased. This observation aligns with microscopic indications of collagen degradation peak 3 days post-ASC interaction. Moreover, a discernible dampening of inflammatory reactions, predominantly neutrophil activation, emerged on day 2, reaching its highest point by day 7 (Fig. 3B).

Finally, the KEGG database showed the "mitigation of Neutrophil extracellular trap pathways" as a highly significant ($P = 4.5 \times 10^{-6}$), suggesting that ASCs modulate the inflammatory cascade via neutrophil activity.

Together, these findings show that ASCs alter the phases of wound healing in culture models.

Identification of TSG-6 as a Prime Candidate for Tissue Remodeling

Next, recognizing remodeling as the result of the interaction of multiple proteins, we hypothesized that the modulation of some driver genes early in the process would lead to an orchestrated remodeling sequence. To

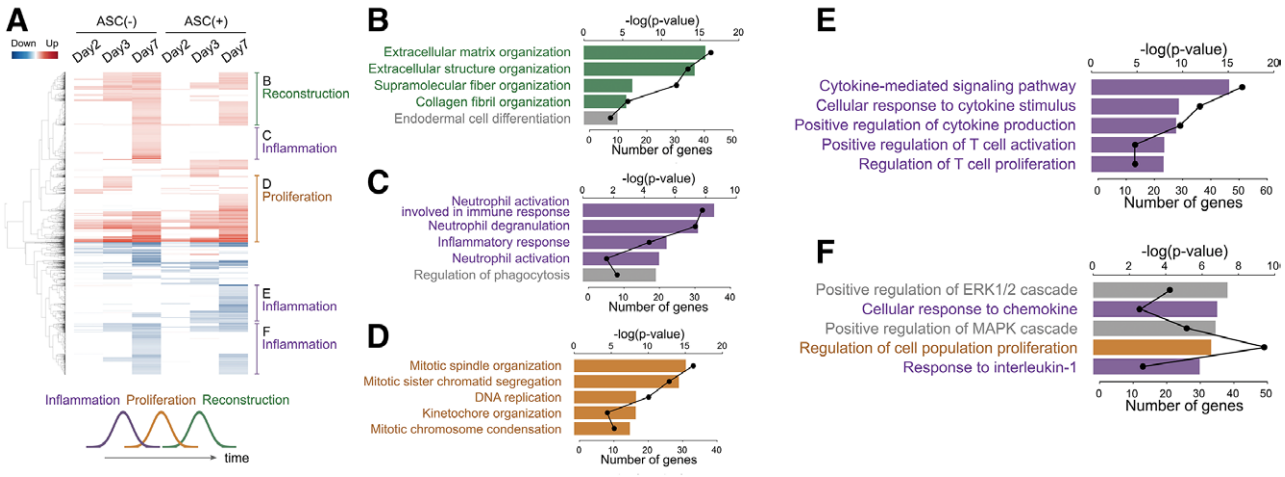

Fig. 2. Analysis of time-series gene expression changes in experimental model. Fresh subcutaneous adipose tissues from five donors (a single replicate per donor) were cultured with or without ASCs. Gene expressions after 1, 2, 3, and 7 days of culture were analyzed by RNA-seq. A, A heatmap of DEGs on each culture day. DEGs were extracted on each culture day against 1 day of culture, using the following criteria: more than 1.5-fold changes and less than 0.05 false discovery rate. Horizontal axis indicates days of culture; vertical axis indicates genes. GO enrichment of each cluster was analyzed and the functions they represent are outlined on the right side. A schematic of the time-series changes is shown at the bottom. B–F, The top five GO biological processes for each cluster, shown in panel A. The bar graph and upper axis represents the negative logarithm of the *P* value. The line graph and lower axis represents the number of DEGs belonging to that category.

identify those driver genes, we built a PPI network of 158 genes that exhibited differential expression after a single day of culture; to enhance the network further, we added other genes that are characteristically expressed in adipose tissue (Fig. 4A).

We assessed which proteins were the most central based on their position and number of neighbors in the network. This use of centrality measures is an established analysis technique, and was used to identify critical genes in multiple biological experiments.[19]

Anticipating the key-regulators to exert influence on surrounding cells, we ranked paracrine factors by their network centralities. Of the 24 candidates, we found that TSG-6 had the highest centrality score (Fig. 4B), and given that it is a prominent antiinflammatory factor secreted by ASCs,[20] we immediately realized its potential role as a chief orchestrator in tissue remodeling.

To validate its role, we used a TSG-6 neutralizing antibody and examined the effects of TSG-6 inhibition on the remodeling response. We assessed fibrous alterations in our experimental model, and type 1 collagen degradation started after 3 days in the ASCs co-culture, whereas only a minor shift was evident in the absence of ASCs. Notably, this ASC-mediated degradation was substantially shortened upon the introduction of the TSG-6 neutralizing antibody (Fig. 5A). Moreover, although type 1 collagen synthesis increased after a 7-day culture irrespective of ASC presence, its amplification was considerably pronounced in the ASC-absent scenario. This increased synthesis under ASC-free conditions is hypothesized to be fibrosis-linked. Furthermore, the potentiation of synthesis by ASCs was markedly impeded by the TSG-6 neutralizing antibody (Fig. 5B), underscoring TSG-6's regulatory role in both degradation and synthesis processes.

Finally, we studied the association between collagen synthesis and fibrosis. We cultured subcutaneous adipose tissues under three distinct conditions: (1) devoid of ASCs, (2) supplemented with ASCs, and (3) combined with both ASCs and the TSG-6 neutralizing antibody. Subsequent qPCR analysis of these tissues revealed a significant downregulation in the α-SMA expression in ASC co-cultures. Importantly, this ASC-induced decline was substantially reversed by the TSG-6 neutralizing antibody, demonstrating the influential role of TSG-6 in the tissue remodeling dynamics (Fig. 5C).

Together, these results demonstrate from different perspectives that TSG-6 is involved in different aspects of tissue remodeling.

TSG-6's Role in Fibrosis Mitigation through NET Suppression

Given that the results from the gene expression analyses showed the downregulation of neutrophil activation by ASCs, we hypothesized that TSG-6 plays a critical role in remodeling via its interaction with NETs.

Assessments on cheek subcutaneous adipose tissue from 15 donors revealed an association between TSG-6 expression and the number of NETs (Fig. 6A). Moreover, we verified NET distribution within ASC co-cultured subcutaneous adipose tissue using immunohistology. Remarkably, the presence of ASCs was associated with a marked decrease in NETs per unit area, underscoring the inhibitory influence of ASCs on NET formation. Interestingly, when the co-culture was supplemented with a TSG-6 neutralizing antibody, the NET count maintained levels comparable to those seen in the absence of ASCs (Fig. 6B). This observation further demonstrates that ASC-mediated suppression of NETs in subcutaneous adipose tissue operates through TSG-6.

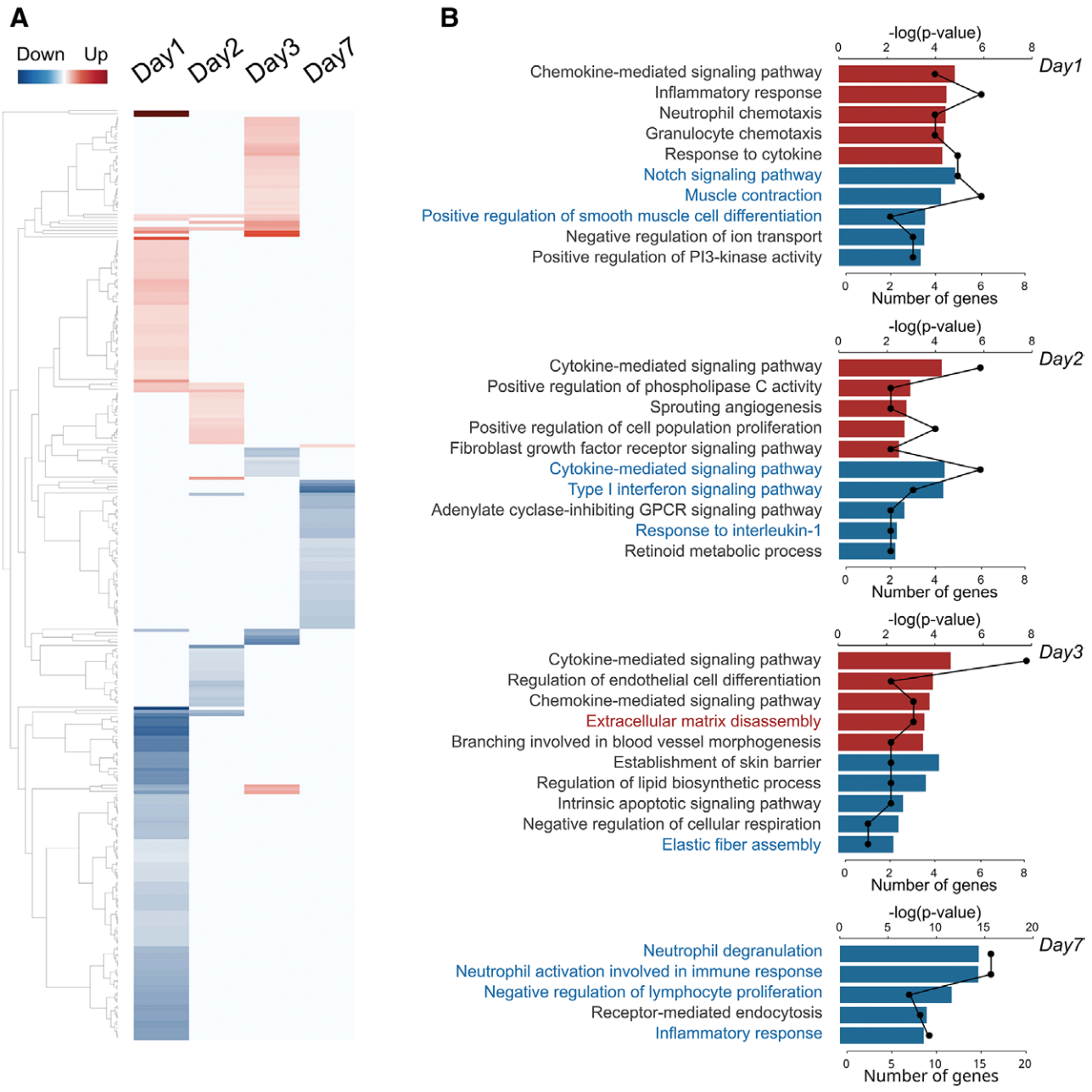

Fig. 3. Analysis of gene expression changes under ASCs influence in experimental model. The same RNA-seq data from Figure 2 was analyzed. A, A heat map of DEGs on each culture day. DEGs were extracted with ASCs compared with without ASCs on each culture day, using the following criteria: more than 1.5-fold changes and less than 0.05 false discovery rate. Horizontal axis indicates days of culture; vertical axis indicates genes. B, Functional analysis of DEGs by GO term on each culture day. For the up- or downregulated genes, the top five GO biological processes were extracted and graphed. Bar graph and upper axis shows the -log of the *P* value. Line graph and lower axis shows the number of DEGs belonging to that category. GO terms mentioned in the text are shown in color.

Finally, we analyzed the impact of NET exposure on the fibrous architecture of the subcutaneous adipose tissue. After 48-hour incubating tissue with NET-laden medium, the expression of both type I collagen and α-SMA was markedly increased (Fig. 6C), suggesting that within subcutaneous adipose tissue, ASCs inhibit NET formation via TSG-6. This seems crucial to steer away the tissue's progression to fibrosis, and toward regenerative remodeling.

DISCUSSION

In this study, we identified TSG-6 as a key factor in tissue remodeling. Using a combination of in silico analyses and ex vivo experiments, we found that TSG-6 exerts its role by reducing NET mobilization, an effect enabled by the presence of ASCs in the subcutaneous adipose tissues culture.

We established an ex vivo model by co-culturing freshly excised human subcutaneous adipose tissue in a

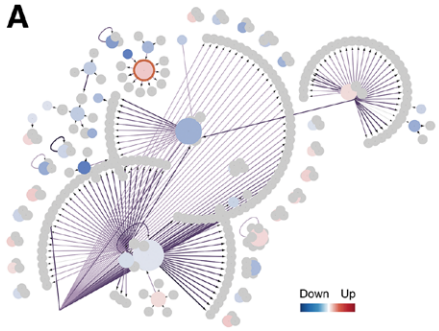

B

Genes	Degree centrality
TSG-6	10
LEP	6
HGF	5
CCL21	3
LOXL4	3
LBP	2
PGF	2

Fig. 4. Biological network analysis to identify a key factor involved in remodeling. A, The PPI network of DEGs on 1 day of ASCs co-culture. Nodes indicate proteins. Edges indicate direct PPI. Node size depends on the number of edges. Red and blue nodes indicate proteins with significantly increased and decreased expression, respectively, whereas gray nodes indicate proteins extracted from the database that bind directly to DEGs in adipose tissue. The color intensity of the edges indicates the reliability of the PPI. TSG-6 is highlighted with framing. B, Ranking of soluble factors with high degree centrality among DEGs after 1 day of culture.

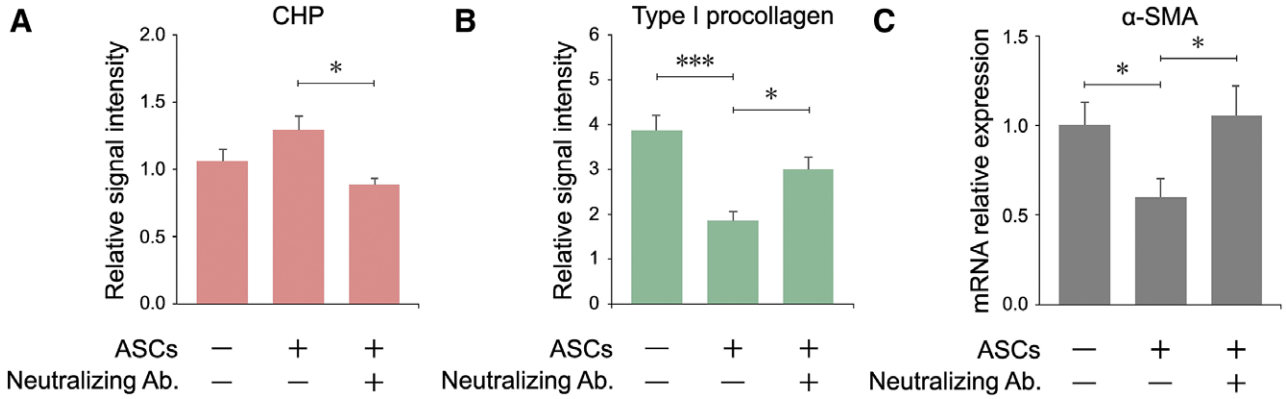

Fig. 5. Verification of the effect of TSG-6 on remodeling. A–B, The observation of fibrous structural changes in ex vivo experimental model when adding TSG-6 neutralizing antibody. Fresh subcutaneous adipose tissue was cultured: without ASCs, with ASCs, and with ASCs and TSG-6 neutralizing antibody. Fluorescent signals of degradation (A) and synthesis (B) of type I collagen were detected before and after culture. Degradation and synthesis were observed after 3 and 7 days, respectively, and the signal intensity of the images was quantified (three donors, each donor n = 5). C, qPCR for a fibrosis-promoting factor. Fresh subcutaneous adipose tissues were cultured: without ASCs, with ASCs, and with ASCs and TSG-6 neutralizing antibody. Tissues were collected after 1 day of culture and subjected to qPCR (three donors, each donor n = 4). Mean and standard error, Tukey HSD test, $*P < 0.05$, $***P < 0.001$.

cell insert with ASCs. This system was used because prevailing theories postulate that the therapeutic prowess of ASC injections may be attributed to the presence of soluble factors[21]; moreover, this model avoids the possibility of ASC-independent reactions, particularly those triggered by physical injection.[22]

This simulates the sequential phases of wound healing, depending on the culture duration. Previous studies have detailed the aftermath of ASC injection into the skin, manifested as tissue trauma, hemorrhage, and inflammation.[23,24] In this light, the tissue we used, derived from living organisms, undoubtedly experienced analogous damage. At the same time, in vivo experiments in animal models would be helpful to further validate and characterize this phenomenon. Furthermore, given the fast start of culturing postharvest, the biological cascade was likely sustained, mirroring the wound healing trajectory in treated skin. A limitation here is the lack of blood circulation, a consequence of culturing excised tissue; hence, it is not possible to establish with certainty whether the effects observed here are due to the inflammatory cells in residual blood of the samples, or more likely, the remaining inflammatory cells resident in the donor tissues. If examined in vivo, we believe the response will be more enhanced due to the presence of migrating blood cells. Nevertheless, the results derived from this model at the tissue, cellular, and molecular levels closely resemble the natural trajectory of tissue remodeling.

A finding from our gene expression analysis was the potential of ASCs to suppress the inflammatory process through TSG-6, suggesting that this factor can reprogram the inflammation stage of wound recovery. During the wound healing progression, the excessive prolongation of the inflammatory phase delays the shift to the proliferative and remodeling phases, and the resulting ECM imbalance sometimes leads to fibrosis.[25–27] Known for their

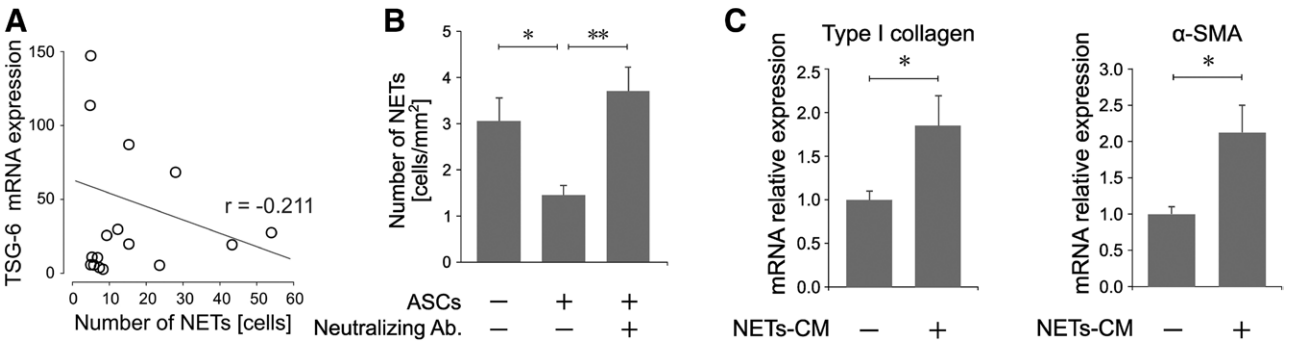

Fig. 6. Analyses of the effect of NETs on fibrous structures of subcutaneous adipose tissue. A, Correlation analysis of TSG-6 expression and the number of NETs in subcutaneous adipose tissue. Each cheek subcutaneous adipose tissue collected from 15 donors was divided into two pieces. One was subjected to qPCR to quantify TSG-6 expression, and the other was immunohistochemically stained to detect and count NETs. TSG-6 mRNA expression and the number of NETs were plotted, and Pearson correlation coefficient (r) was calculated. B, Numbers of NETs in immunohistochemical staining images. Fresh subcutaneous adipose tissues were cultured under the following three conditions: without ASCs, with ASCs, and with ASCs and TSG-6 neutralizing antibody. Tissues were immunohistochemically stained after 1 day of culture and NETs were counted (four donors, each donor n = 6). Mean and standard error, Tukey HSD test, $*P < 0.05$, $**P < 0.01$. C, Effect of NETs on fibrosis-related gene expression in subcutaneous adipose tissue. NETs were induced in neutrophils, and the culture supernatant containing NETs was collected. Expression of fibrosis-related genes in fresh subcutaneous adipose tissue cultured with the supernatant containing NETs was quantified by qPCR. Of the four donors evaluated, the results of a single representative donor are presented (four donors, each donor n = 4). CM; conditioned medium. Mean and standard error, paired *t* test, $*P < 0.05$.

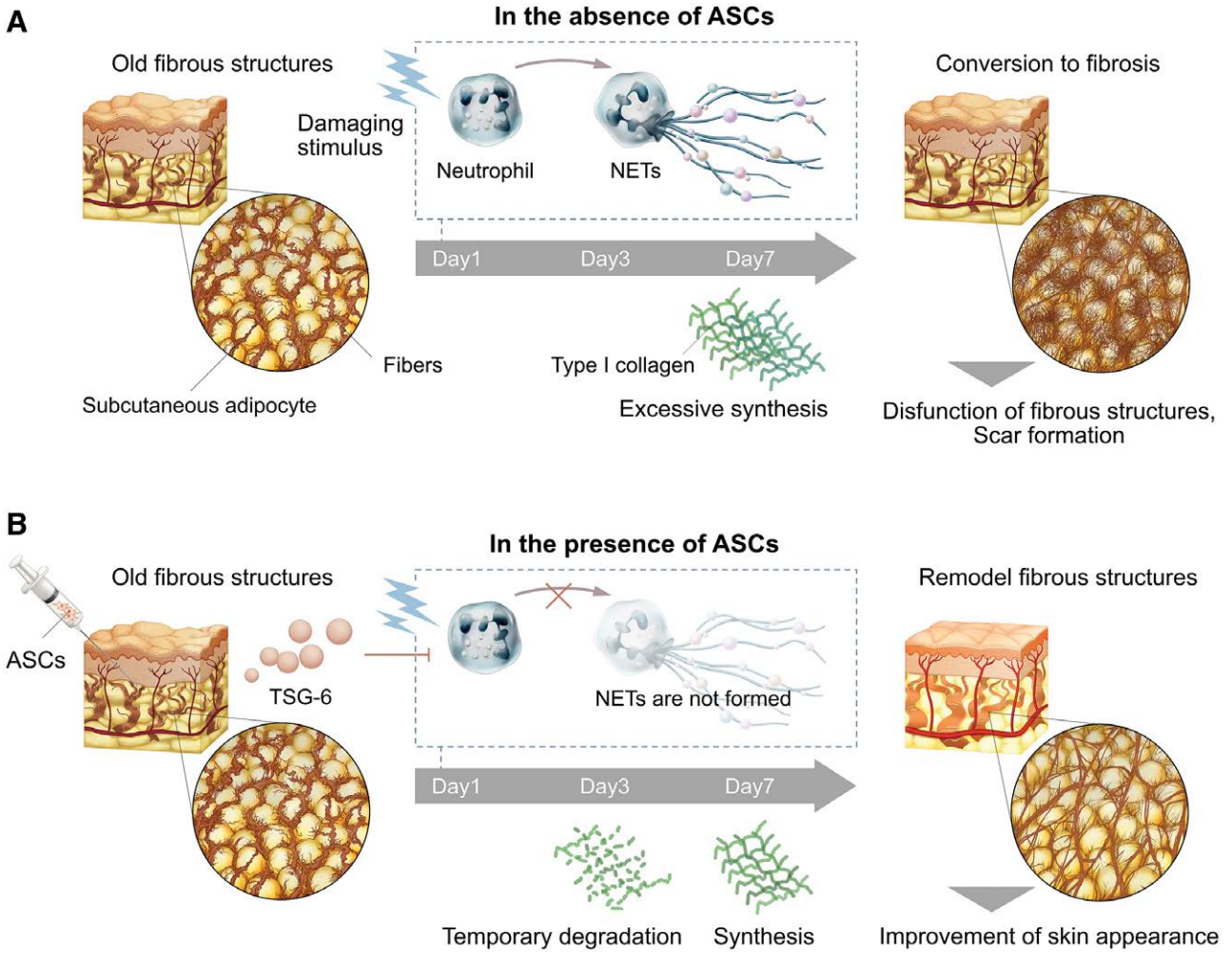

Fig. 7. Conceptual diagram of this study. A, In the absence of ASCs, neutrophils form NETs in damaged subcutaneous adipose tissue; NETs cause excessive synthesis of type I collagen and mediate the transition to fibrosis. B, In the presence of ASCs, TSG-6 released from ASCs inhibits the formation of NETs. This induces transient degradation and subsequent synthesis of type I collagen resulting in tissue remodeling.

immunomodulatory prowess, ASCs likely act in preventing excessive inflammation during wound recovery.[28–30] One of the prominent antiinflammatory factors secreted by ASCs is TSG-6, whose effect has been documented to influence multiple immune cells,[31–33] and linked to wound closure and fibrosis suppression in murine models by genetic deletion experiments of TSG-6[34]; this is consistent with our observations of the role of TSG-6.

In this sense, upon tissue damage, neutrophils mobilize to form NETs, structures that release intracellular substances such as chromatin skeletons and granulocyte proteins into the extracellular space.[35] Although this is one of the biological defense systems, NET overproduction has been linked to chronic inflammation and fibrosis.[36] Our findings suggest that NETs are involved in one of the inflammatory processes in the subcutaneous adipose tissue, and that TSG-6 is a master regulator of its activity (Fig. 7). These results point toward the next step in research involving tissue remodeling, namely a detailed clarification of the mechanism underlying neutrophil mobilization and NETs in human skin undergoing aesthetic treatment.

In summary, we found that in subcutaneous adipose tissue, TSG-6 inhibits the release of NETs, steering the tissue towards a beneficial remodeling and avoiding fibrosis. Regulation of TSG-6 may shorten the recovery time after aesthetic treatments and allow patients to obtain maximum rejuvenation effects. Its modulation can lead to the establishment of aesthetic procedures that do not require subcutaneous injection of cells.

CONCLUSION

TSG-6 is a key factor that modulates inflammation by inhibiting the formation of NETs in subcutaneous adipose tissue.

Satomi Kiuchi, MS
Frontier Research Center
POLA Chemical Industries, Inc.
560 Kashio-cho, Totsuka-ku
Yokohama, Japan
E-mail: s-kiuchi@pola.co.jp

DISCLOSURES

Kiuchi is an author on a patent applied for by POLA Chemical Industries that relates to this study. All the other authors have no financial interest to declare in relation to the content of this article. This study was funded by POLA Chemical Industries, Inc.

REFERENCES

1. Mora Huertas AC, Schmelzer CEH, Hoehenwarter W, et al. Molecular-level insights into aging processes of skin elastin. *Biochimie*. 2016;128-129:163–173.
2. Varani J, Spearman D, Perone P, et al. Inhibition of type I procollagen synthesis by damaged collagen in photoaged skin and by collagenase-degraded collagen in vitro. *Am J Pathol*. 2001;158:931–942.
3. Varani J, Dame MK, Rittie L, et al. Decreased collagen production in chronologically aged skin: roles of age-dependent alteration in fibroblast function and defective mechanical stimulation. *Am J Pathol*. 2006;168:1861–1868.
4. Charles-de-Sa L, Gontijo-de-Amorim NF, Maeda Takiya C, et al. Antiaging treatment of the facial skin by fat graft and adipose-derived stem cells. *Plast Reconstr Surg*. 2015;135:999–1009.
5. Luan A, Duscher D, Whittam AJ, et al. Cell-assisted lipotransfer improves volume retention in irradiated recipient sites and rescues radiation-induced skin changes. *Stem Cells*. 2016;34:668–673.
6. Yoshimura K. Regenerative medicine with adipose stem/progenitor cells: application to cosmetic dermatology. *Aesthet Dermatol*. 2010;20:225–236.
7. Andrews S. FastQC: a quality control tool for high throughput sequence data. Available at https://www.bioinformatics.babraham.ac.uk/projects/fastqc/. Published 2010. Accessed June 13, 2024.
8. Kim D, Langmead B, Salzberg SL. HISAT: a fast spliced aligner with low memory requirements. *Nat Methods*. 2015;12:357–360.
9. Mortazavi A, Williams BA, McCue K, et al. Mapping and quantifying mammalian transcriptomes by RNA-Seq. *Nat Methods*. 2008;5:621–628.
10. Love MI, Huber W, Anders S. Moderated estimation of fold change and dispersion for RNA-seq data with DESeq2. *Genome Biol*. 2014;15:550.
11. Chen EY, Tan CM, Kou Y, et al. Enrichr: interactive and collaborative HTML5 gene list enrichment analysis tool. *BMC Bioinf*. 2013;14:128.
12. Kuleshov MV, Jones MR, Rouillard AD, et al. Enrichr: a comprehensive gene set enrichment analysis web server 2016 update. *Nucleic Acids Res*. 2016;44:W90–W97.
13. Alanis-Lobato G, Andrade-Navarro MA, Schaefer MH. HIPPIE v2.0: enhancing meaningfulness and reliability of protein-protein interaction networks. *Nucleic Acids Res*. 2017;45:D408–D414.
14. Shannon P, Markiel A, Ozier O, et al. Cytoscape: a software environment for integrated models of biomolecular interaction networks. *Genome Res*. 2003;13:2498–2504.
15. Schopow N, Kallendrusch S, Gong S, et al. Examination of ex-vivo viability of human adipose tissue slice culture. *PLoS One*. 2020;15:e0233152.
16. Martin P. Wound healing–aiming for perfect skin regeneration. *Science*. 1997;276:75–81.
17. Condorelli AG, El Hachem M, Zambruno G, et al. Notch-ing up knowledge on molecular mechanisms of skin fibrosis: focus on the multifaceted Notch signaling pathway. *J Biomed Sci*. 2021;28:36.
18. Hinz B. Myofibroblasts. *Exp Eye Res*. 2016;142:56–70.
19. Alm E, Arkin AP. Biological networks. *Curr Opin Struct Biol*. 2003;13:193–202.
20. Lee RH, Yu JM, Foskett AM, et al. TSG-6 as a biomarker to predict efficacy of human mesenchymal stem/progenitor cells (hMSCs) in modulating sterile inflammation in vivo. *Proc Natl Acad Sci USA*. 2014;111:16766–16771.
21. Kim WS, Park BS, Sung JH. Protective role of adipose-derived stem cells and their soluble factors in photoaging. *Arch Dermatol Res*. 2009;301:329–336.
22. Robertson R, Broers B, Harris M. Injecting drug use, the skin and vasculature. *Addiction*. 2021;116:1914–1924.
23. Yoshimura K, Suga H, Eto H. Adipose-derived stem/progenitor cells: roles in adipose tissue remodeling and potential use for soft tissue augmentation. *Regen Med*. 2009;4:265–273.
24. Suga H, Eto H, Shigeura T, et al. IFATS collection: fibroblast growth factor-2-induced hepatocyte growth factor secretion by adipose-derived stromal cells inhibits postinjury fibrogenesis through a c-Jun N-terminal kinase-dependent mechanism. *Stem Cells*. 2009;27:238–249.
25. Loots MA, Lamme EN, Zeegelaar J, et al. Differences in cellular infiltrate and extracellular matrix of chronic diabetic and venous ulcers versus acute wounds. *J Invest Dermatol*. 1998;111:850–857.
26. Wynn TA, Ramalingam TR. Mechanisms of fibrosis: therapeutic translation for fibrotic disease. *Nat Med*. 2012;18:1028–1040.

27. Wick G, Grundtman C, Mayerl C, et al. The immunology of fibrosis. *Annu Rev Immunol.* 2013;31:107–135.
28. Baharlou R, Ahmadi-Vasmehjani A, Faraji F, et al. Human adipose tissue-derived mesenchymal stem cells in rheumatoid arthritis: regulatory effects on peripheral blood mononuclear cells activation. *Int Immunopharmacol.* 2017;47:59–69.
29. Anderson P, Gonzalez-Rey E, O'Valle F, et al. Allogeneic adipose-derived mesenchymal stromal cells ameliorate experimental autoimmune encephalomyelitis by regulating self-reactive T cell responses and dendritic cell function. *Stem Cells Int.* 2017;2017:2389753.
30. Franquesa M, Mensah FK, Huizinga R, et al. Human adipose tissue-derived mesenchymal stem cells abrogate plasmablast formation and induce regulatory B cells independently of T helper cells. *Stem Cells.* 2015;33:880–891.
31. Song WJ, Li Q, Ryu MO, et al. TSG-6 secreted by human adipose tissue-derived mesenchymal stem cells ameliorates DSS-induced colitis by inducing M2 macrophage polarization in mice. *Sci Rep.* 2017;7:5187.
32. Mittal M, Tiruppathi C, Nepal S, et al. TNFalpha-stimulated gene-6 (TSG6) activates macrophage phenotype transition to prevent inflammatory lung injury. *Proc Natl Acad Sci.* 2016;113:E8151–E8158.
33. Dyer DP, Thomson JM, Hermant A, et al. TSG-6 inhibits neutrophil migration via direct interaction with the chemokine CXCL8. *J Immunol.* 2014;192:2177–2185.
34. Qi Y, Jiang D, Sindrilaru A, et al. TSG-6 released from intradermally injected mesenchymal stem cells accelerates wound healing and reduces tissue fibrosis in murine full-thickness skin wounds. *J Invest Dermatol.* 2014;134:526–537.
35. Brinkmann V, Reichard U, Goosmann C, et al. Neutrophil extracellular traps kill bacteria. *Science.* 2004;303:1532–1535.
36. Chrysanthopoulou A, Mitroulis I, Apostolidou E, et al. Neutrophil extracellular traps promote differentiation and function of fibroblasts. *J Pathol.* 2014;233:294–307.